Electronic Supplementary Material (ESI) for Journal of Materials Chemistry C.

Supporting Information

Phase Dependent Visible to Near-Infrared Photoluminescence of $CuInS_2$ Nanocrystals

A. D. P. Leach, L. G. Mast, E. A. Hernandez-Pagan and J. E. Macdonald*

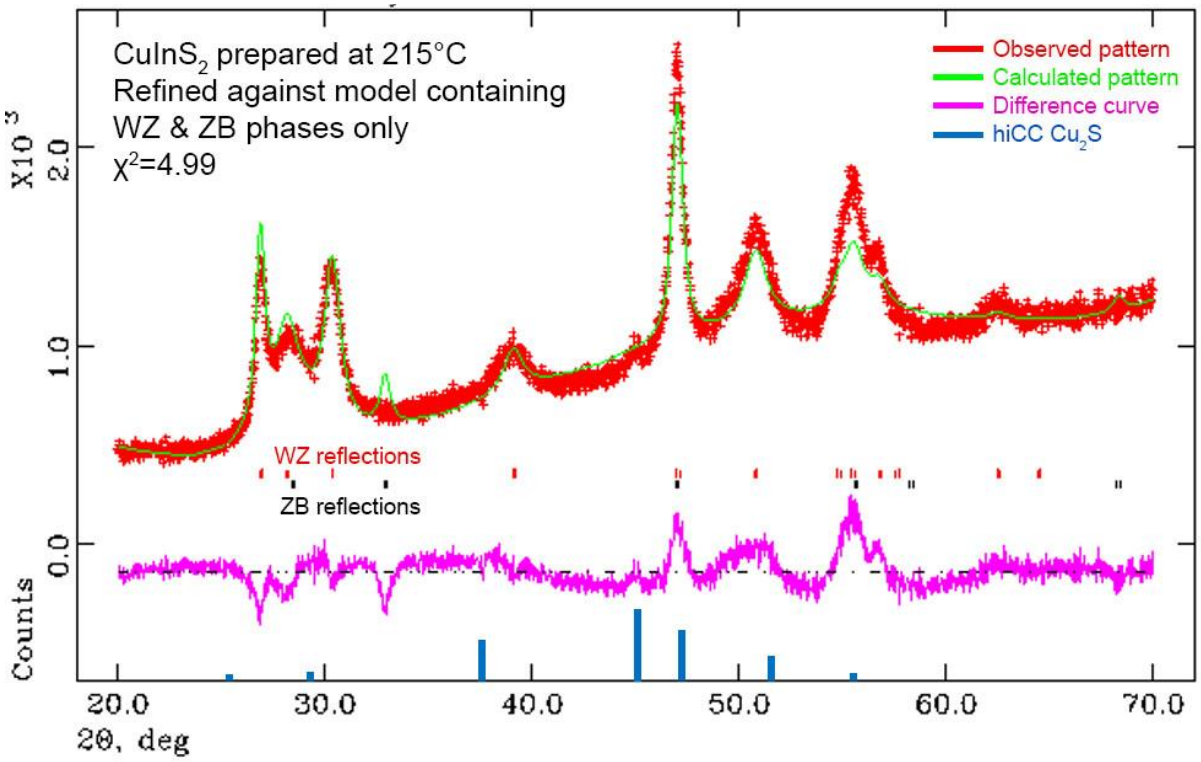

Figure S1. Rietveld Refinement for $CuInS_2$ sample prepared at 215°C using a model of the $CuInS_2$ ZB & WZ structures only. The reflections for hiCC Cu_2S (JCPDS card no. 46-1195) are shown below (blue) and are in good agreement with large peaks in the difference curve (pink).

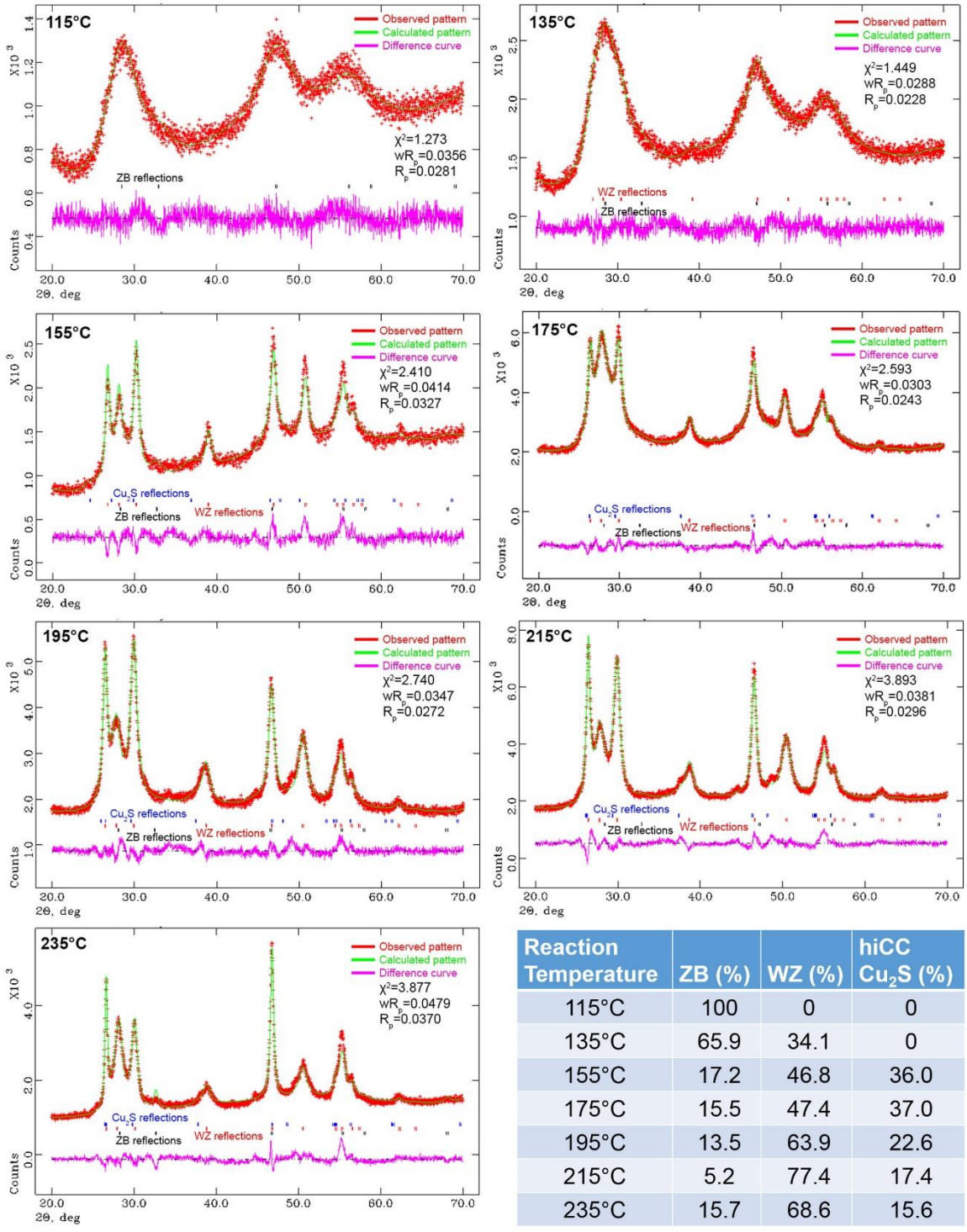

Reaction Temperature	ZB (%)	WZ (%)	hiCC Cu_2S (%)
115°C	100	0	0
135°C	65.9	34.1	0
155°C	17.2	46.8	36.0
175°C	15.5	47.4	37.0
195°C	13.5	63.9	22.6
215°C	5.2	77.4	17.4
235°C	15.7	68.6	15.6

Figure S2. Rietveld Refinements for samples prepared from 115 - 235°C. Reflections for each phase in the model are shown between the experimental and difference curves. *Note*: at 115°C the model only contains the ZB $CuInS_2$ phase; at 135°C the model contains only the ZB & WZ $CuInS_2$ phases. Phase content values (%) are shown at the bottom right.

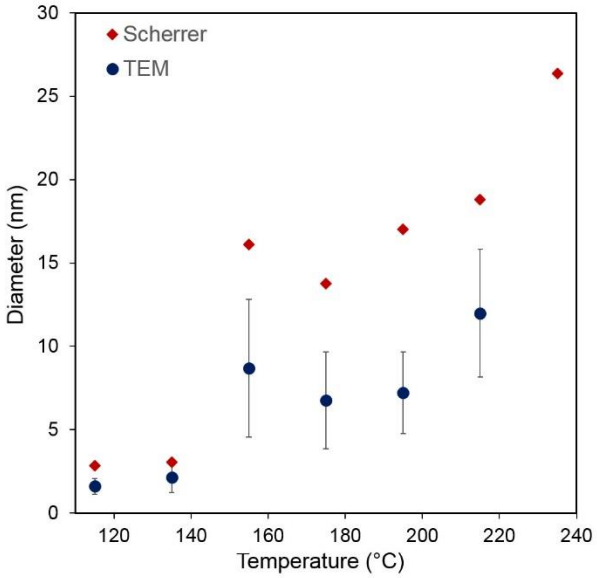

Figure S3. The variation in spherical/plate-like NC diameter calculated from TEM images (blue) and the Scherrer line broadening equation *via* XRD (red) plotted as a function of temperature. Error bars show the standard deviation. The diameter of rod shaped NCs measured from TEM images is not plotted.

Reaction Temperature	Cu : In : S Ratio
115°C	1.4 : 1 : 19.3
135°C	5.3 : 1 :15.0
155°C	1.0 : 1 : 3.1
175°C	1.4 : 1 : 3.7
195°C	1 : 1.0 : 3.8
215°C	2.7 : 1 : 2.0
235°C	1.1 : 1 : 1.93

Figure S4. EDS data collected from samples prepared from 115 - 235°C. This indicates the ensemble elemental composition of each sample. This data is of limited significance given the multitude of phases identified in the final product as well as the potential for unreacted reagents in the product at lower temperatures. However, in general, as the reaction temperature increases, samples become closer in stoichiometry to $CuInS_2$.

Reaction Temperature	QY (%)
115°C	0.05
135°C	0.06
155°C	0.11
175°C	0.45
195°C	0.76
215°C	0.42
235°C	0.04

Figure S5. Table showing the quantum yield (QY) as a percentage value for each sample calculated using the PL spectra shown in Figure 4c. The QY was determined for each sample by comparison to a Rh-101 standard. All samples have QY < 1%.

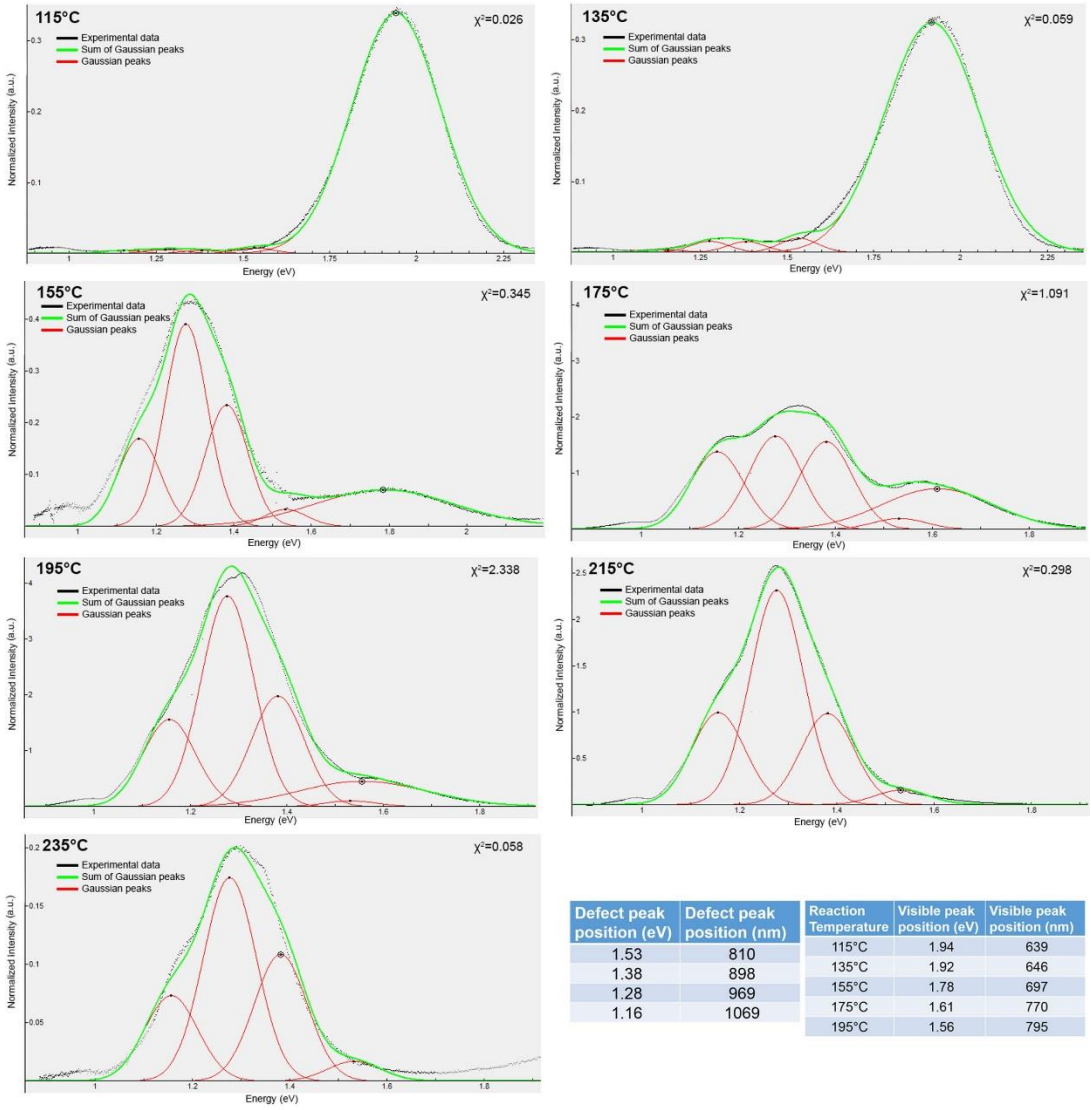

Defect peak position (eV)	Defect peak position (nm)
1.53	810
1.38	898
1.28	969
1.16	1069

Reaction Temperature	Visible peak position (eV)	Visible peak position (nm)
115°C	1.94	639
135°C	1.92	646
155°C	1.78	697
175°C	1.61	770
195°C	1.56	795

Figure S6. PL data (black), showing intensity vs. energy in eV, for samples prepared at reaction temperature (115-235°C) fit with Gaussian peaks (red) using Fityk, a curve fitting and data analysis application. Data were fit to within a statistically acceptable tolerance ($\chi^2 \leq 2.4$) with four peaks in the NIR region and one peak in the visible region. The sum of the fitted peaks is shown (green). Fit was initially performed on data obtained for reaction at 215°C, as no peak in the visible was observed here allowing only WZ emission to be considered. The spectral position of the NIR peaks (in eV and nm) is shown at the bottom right (left hand side). FWHM (0.12 eV) and peak positions of the Gaussians were then fixed and these curves were fit to PL data at each reaction temperature. At reaction temperatures ≤ 195°C a further Gaussian peak in the visible region was added to account for the emission of the ZB phase. The position of this

peak increased in wavelength with temperature and is shown in the table at the bottom right (right hand side).

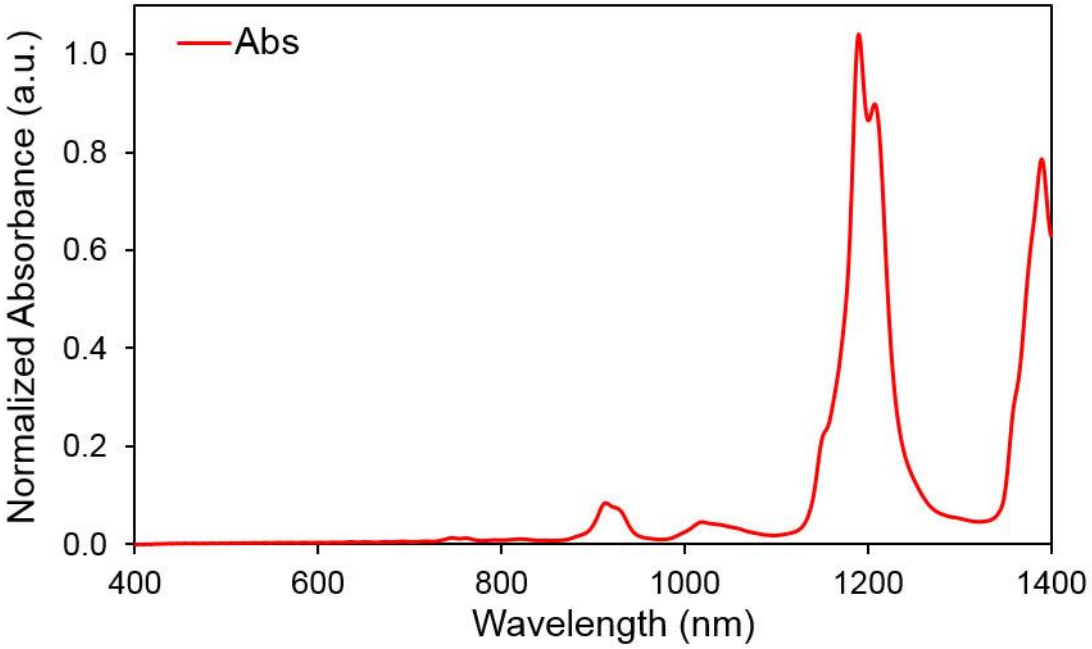

Figure S7. Absorbance spectra of hexanes. The intense peak at 1200 nm causes the re-absorbance of emitted light from $CuInS_2$ samples that fluoresce in this region. It should be therefore be noted that the decrease in PL intensity observed at ~ 1200 nm in all samples is due to the re-absorbance of emitted light by the solvent hexanes.[1] Given the nature of this absorbance, PL data is fit excluding the region from 1130 – 1290 nm.

1 A. Aharoni, D. Oron, U. Banin, E. Rabani, J. Jortner, *Physical Review Letters*, 2008, **100**.

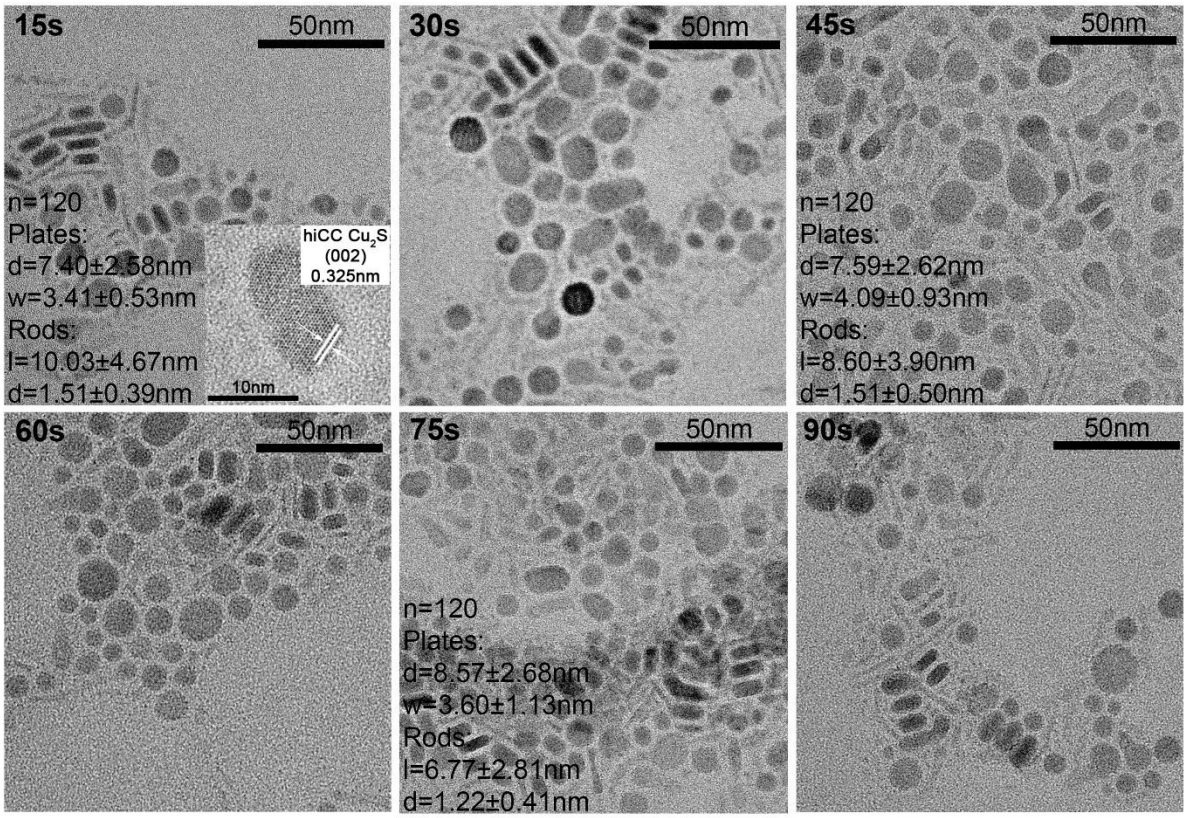

Figure S8. TEM images of aliquots taken 15s, 30s, 45s, 60s, 75s and 90s after injection of the Cu—thiolate complex at reaction temperature 215°C. Inset in the 15s image is an HRTEM image showing lattice fringing characteristic of hiCC Cu_2S.[2] Images were sized every 30s.

2 J.-Y. Chang, C.-Y. Cheng, *Chemical Communications*, 2011, **47**, 9089.

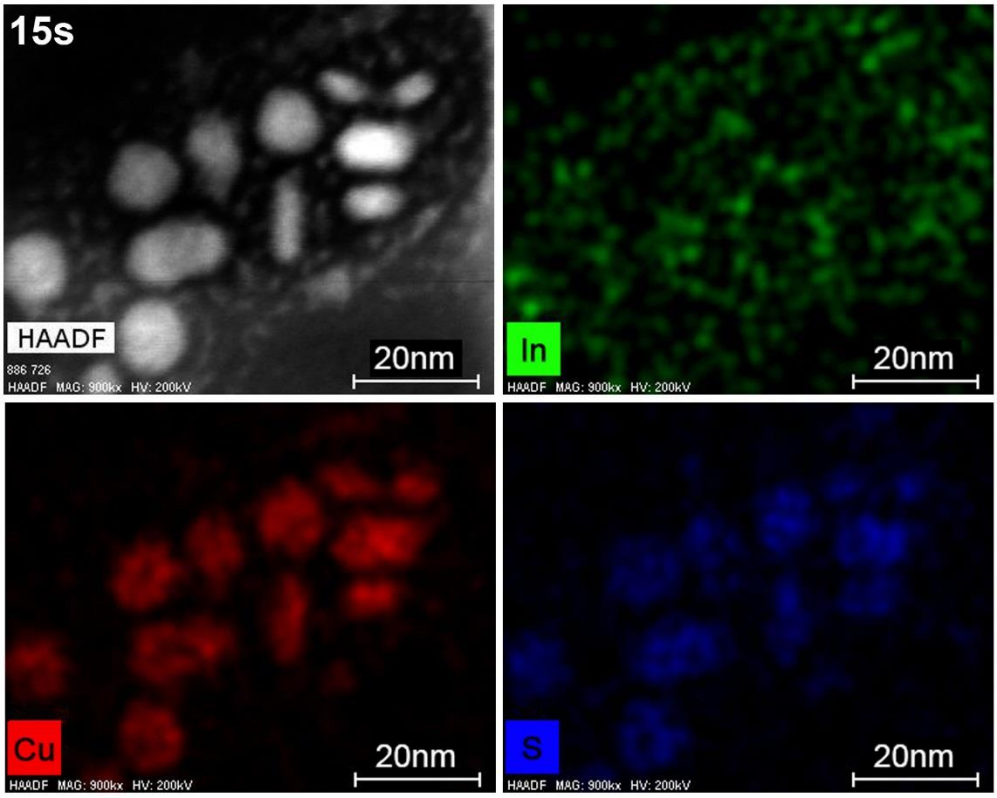
15s
HAADF
886 726
HAADF MAG: 900kx HV: 200kV
20nm
In
HAADF MAG: 900kx HV: 200kV
20nm
Cu
HAADF MAG: 900kx HV: 200kV
20nm
S
HAADF MAG: 900kx HV: 200kV
20nm

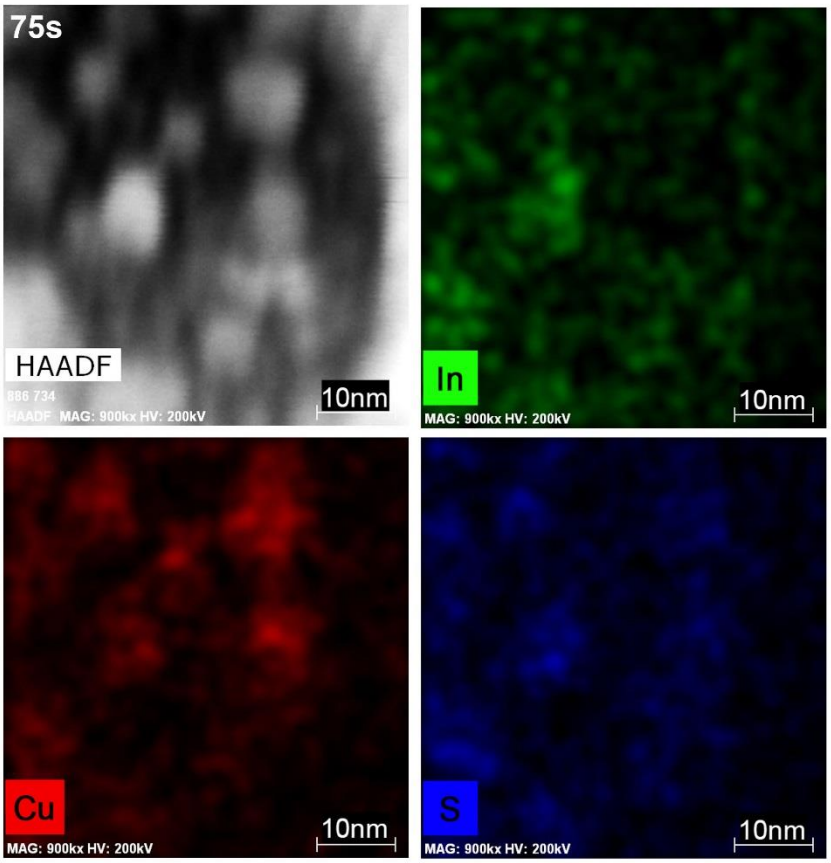
75s
HAADF
886 734
HAADF MAG: 900kx HV: 200kV
10nm
In
MAG: 900kx HV: 200kV
10nm
Cu
MAG: 900kx HV: 200kV
10nm
S
MAG: 900kx HV: 200kV
10nm

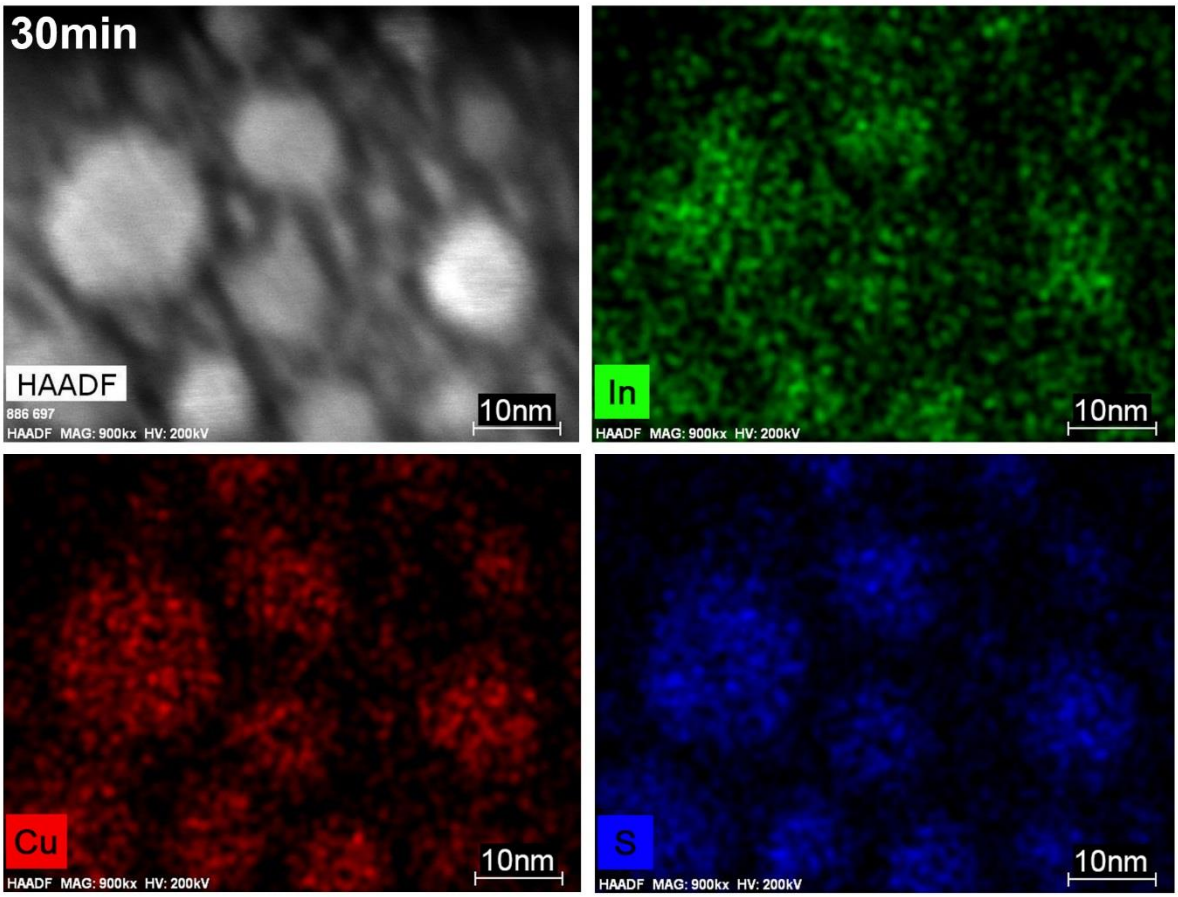

Figure S9. HAADF (high-angle annular dark field) images and single elemental analysis of the EDS maps shown in Figure 7.